



Article

# A Shadowed Type-2 Fuzzy Approach for Crossover Parameter Adaptation in Differential Evolution

**Patricia Ochoa** <sup>1</sup>, **Cinthia Peraza** <sup>1</sup> , **Oscar Castillo** <sup>1</sup> and **Zong Woo Geem** <sup>2,\*</sup>

<sup>1</sup> Tijuana Institute of Technology, TecNM, Calzada Tecnológico s/n, Fracc. Tomas Aquino, Tijuana 22379, Mexico; martha.ochoa18@tectijuana.edu.mx (P.O.); cinthia.peraza@tectijuana.edu.mx (C.P.); ocastillo@tectijuana.mx (O.C.)

<sup>2</sup> College of IT Convergence, Gachon University, Seongnam 13120, Republic of Korea

\* Correspondence: geem@gachon.ac.kr

**Abstract:** The shadowed type-2 fuzzy systems are used more frequently today as they provide an alternative to classical fuzzy logic. The primary purpose of fuzzy logic is to simulate reasoning in a computer. This work aims to use shadowed type-2 fuzzy systems (ST2-FS) to dynamically adapt the crossing parameter of differential evolution (DE). To test the performance of the dynamic crossing parameter, the motor position control problem was used, which contains an interval type-2 fuzzy system (IT2-FS) for controlling the motor. A comparison is made between the original DE and the algorithm using shadowed type-2 fuzzy systems (DE-ST2-FS), as well as a comparison with the results of other state-of-the-art metaheuristics.

**Keywords:** shadowed type-2 fuzzy logic; interval type-2 fuzzy controller; differential evolution



**Citation:** Ochoa, P.; Peraza, C.; Castillo, O.; Geem, Z.W. A Shadowed Type-2 Fuzzy Approach for Crossover Parameter Adaptation in Differential Evolution. *Algorithms* **2023**, *16*, 279. <https://doi.org/10.3390/a16060279>

Academic Editors: Ramiro Barbosa, Paulo Moura Oliveira and Frank Werner

Received: 24 April 2023

Revised: 26 May 2023

Accepted: 29 May 2023

Published: 31 May 2023



**Copyright:** © 2023 by the authors. Licensee MDPI, Basel, Switzerland. This article is an open access article distributed under the terms and conditions of the Creative Commons Attribution (CC BY) license (<https://creativecommons.org/licenses/by/4.0/>).

## 1. Introduction

Fuzzy logic is a modern tool, and one of its most important applications is process control. It has shown rapid growth as it can solve problems related to information or knowledge uncertainty, providing a formal method for expressing knowledge in a way that is understandable for humans. It uses linguistic variables for this purpose.

The success of applying fuzzy logic is primarily due to its ability to utilize ambiguous concept models, which helps in reducing the intuitive complexity of a process. This allows for control operations to be carried out, albeit in an approximate or heuristic manner, on nonlinear or time-varying processes [1–5].

Fuzzy logic has achieved significant success in industrial control. While there are various versions of controllers that employ fuzzy logic, the term “fuzzy controller” typically refers to a control system with an internal structure that includes a fuzzy system to govern the controller. One of the frequently mentioned advantages of fuzzy controllers, in comparison to other controller types, is their ability to be designed even in the absence of an exact model of the plant to be controlled, as they are rule-based [6–15].

A new type of fuzzy sets of higher order, known as type-2 fuzzy sets, was proposed by Zadeh in 1975 as an enhancement to fuzzy sets. These sets can handle system uncertainties by considering degrees of membership. The literature demonstrates the development of numerous works that utilize type-2 fuzzy controllers, which exhibit improved results [16–25]. Therefore, in this work, an interval type-2 fuzzy controller is implemented for this reason.

Similarly, this work also presents the utilization of shadowed type-2 fuzzy systems, which represent an alternative branch in fuzzy logic. The concept of shadowed sets was originally introduced to enhance the interpretability of type-1 fuzzy sets and address the issues of excessive precision [26–30]. In this work, ST2-FSs will be employed to dynamically adapt the crossover parameter (CR) of differential evolution, with the primary objective of improving the results.

The aforementioned aims to demonstrate the significance of this development, wherein the CR parameter is dynamically utilized in DE. Few works in the literature showcase the performance of the dynamic CR parameter, hence emphasizing the main reason for its adoption. Furthermore, we have an interval type-2 fuzzy system controller for the motor, which is commonly employed in the state-of-the-art technologies. Moreover, this work presents the integration of these two concepts to validate the potential of their combined application and assess their effectiveness.

The contribution of this article is to utilize a novel approach, shadowed type-2 fuzzy systems (ST2-FS), for dynamically adapting the crossover parameter of differential evolution (DE), in this way obtaining a new variant of DE. This adaptation aims to enhance the performance of the DE algorithm when applied to the optimization of the motor position control problem with interval type-2 fuzzy logic.

This paper provides the following content: Section 2 presents the definition of ST2-FSs, Section 3 introduces the DE theory, Section 4 describes the utilization of the DE algorithm with shadowed fuzzy, Section 5 presents the controller, Section 6 outlines the Results, and Section 7 concludes the paper.

## 2. Shadowed Type-2 Fuzzy Systems

Fuzzy logic, initiated in 1965 [31,32], is mainly based on the way we perceive the world that cannot always be defined in terms of true or false sentences, that is, it is logically applied to concepts that can take a value and any truth within a set of values.

The evolution of fuzzy logic over time was type-1 fuzzy systems (T1-FS), then intervals type-2 fuzzy systems (IT2-FS), and later generalized type-2 fuzzy systems (GT2-FS); the mathematical equations of each of these systems are presented in Equations (1)–(3) respectively:

$$\tilde{A} = \{(x, \mu_A(x)) | x \in U, [0, 1]\} \quad (1)$$

In Equation (2)  $J_x$  is referred to the primary membership of  $x$  in  $\tilde{A}$ . For each value of  $x$ , denoted as  $x = x'$ , the two-dimensional (2D) plane formed by the axes  $u$  and  $\mu_{\tilde{A}}(x', u)$  is known as a vertical slice of  $\tilde{A}$ .

A secondary membership function corresponds to a vertical slice of  $\tilde{A}$ , denoted as  $\mu_{\tilde{A}}(x', u)$ , where  $x' \in X$  and  $\forall u \in J_{x'} \subseteq [0, 1]$ . It can be described as follows:

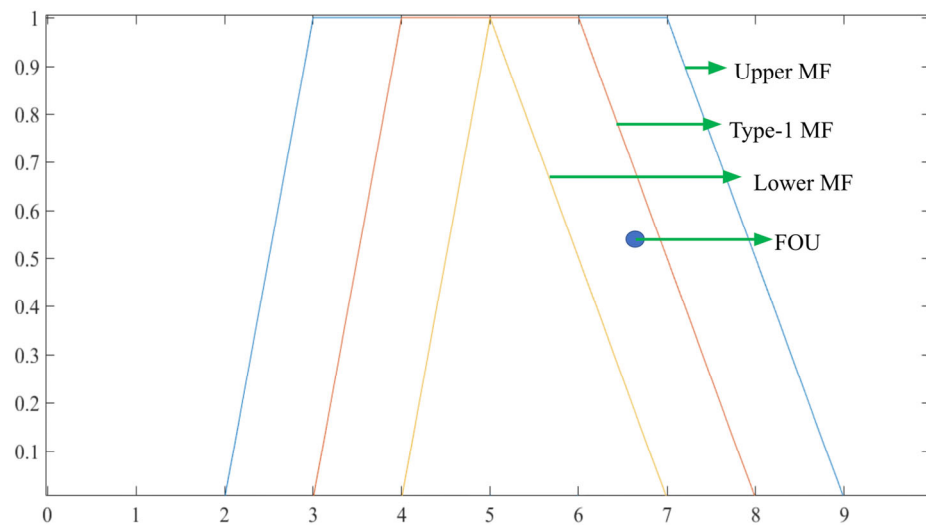
$$\tilde{A} = \{(x, u), \mu_{\tilde{A}}(x, u) | \forall x \in X, \forall u \in J_x \subseteq [0, 1]\} \quad (2)$$

A generalized type-2 fuzzy set, denoted by  $\tilde{\tilde{A}}$ , is defined by a type-2 membership function  $\mu_{\tilde{\tilde{A}}}(x, u)$ , where  $x \in X, u \in J_x \subseteq [0, 1]$ , and  $0 \leq \mu_{\tilde{\tilde{A}}}(x, u) \leq 1$ . It can be represented by:

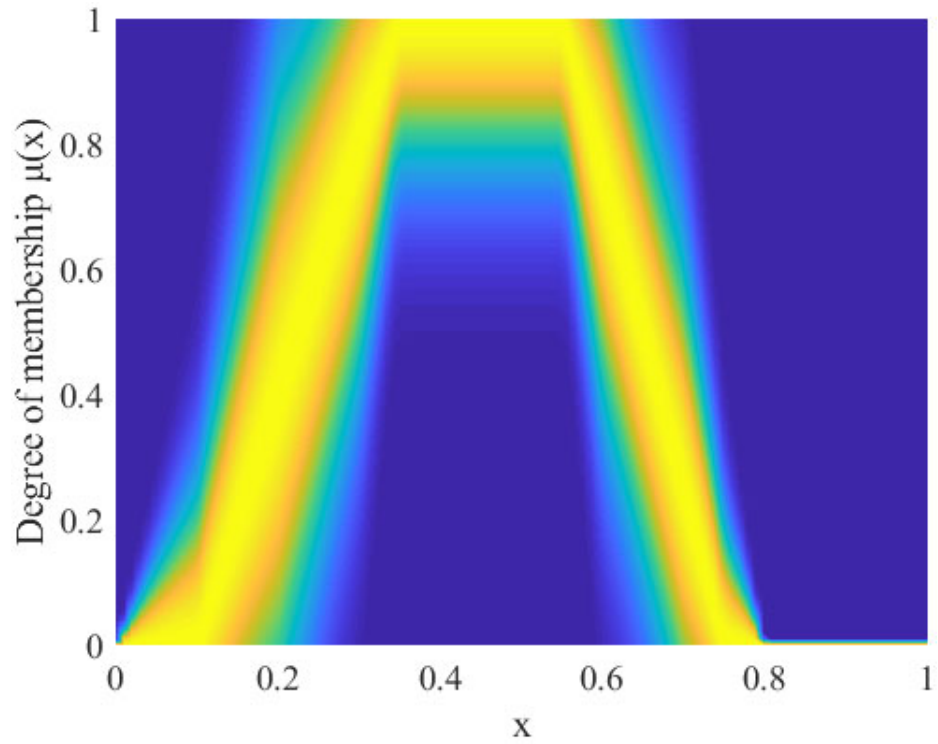
$$\tilde{\tilde{A}} = \left\{ \left( (x, u), \mu_{\tilde{\tilde{A}}}(x, u) \right) \mid \forall x \in X, \forall u \in J_x^u \subseteq [0, 1] \right\} \quad (3)$$

Figure 1 depicts the type-1 and interval type-2 fuzzy sets, while Figure 2 illustrates the generalized type-2 fuzzy set, where the orange and yellow colors represent the primary membership function of a trapezoidal, the green color represents the secondary membership function of a Gaussian, and finally the blue color represents the fraction of uncertainty of the kernel and the support of the secondary membership function respectively.

It is widely recognized that the utilization of generalized fuzzy systems entails a significant computational cost for their execution. In order to mitigate this, alternative approaches have been proposed that offer lower computational overhead. These alternatives include Z slices or vertical slices, as well as geometric approximations [33]. Additionally, the literature presents another option known as horizontal sections or  $\alpha$ -representation of planes [34–36].



**Figure 1.** Illustration of the type-1 and interval type-2 fuzzy sets.



**Figure 2.** Illustration of the general type-2 fuzzy set.

Taking into account the alternatives discussed in the literature, this paper investigates the utilization of  $\alpha$ -planes. Equations (4) and (5) outline the structure of an  $\alpha$ -plane and the combination of an IT2-FIS with an  $\alpha$ -plane to model a GT2-FS, respectively.

$$\tilde{A}_\alpha = \{(x, u), \alpha) | \forall x \in X, \forall u \in J_x \subseteq [0, 1]\} \quad (4)$$

$$\tilde{\tilde{A}} = \bigcup \tilde{A}_\alpha \quad (5)$$

The elimination of excessive precision is one of the main ones that is sought to be carried out when using a ST2-FS, since this helps to reduce the computational cost. To achieve the elimination of excessive precision, a GT2-FS is modeled using only 2  $\alpha$ -planes; this idea was

proposed in Pedrycz concepts, thus creating the theory of shadowed sets [37–40], where the main contribution is the creation of optimal  $\alpha$ -planes.

Equation (6) explains the mathematical form of the shadowed sets; this formula is built from 2  $\alpha$ -cuts on a T1-FS, with  $\alpha$  and  $\beta$  values, producing three intervals.

$$S_{\mu_A}(x) = \begin{cases} 1, & \text{if } \mu_A(x) \geq \alpha \\ 0, & \text{if } \mu_A(x) \leq \beta \\ [0, 1], & \text{if } \alpha \leq \mu_A(x) \geq \beta \end{cases} \quad (6)$$

According to the theory of shadowed sets, optimal values for the variables  $\alpha$  and  $\beta$  are proposed, which can be computed using Equation (7). Figure 3 illustrates the process of obtaining the values of  $\alpha$  and  $\beta$ , along with the three corresponding areas: the raised area, the reduced area, and the shaded area. Each area is represented by a different color.

$$\text{elevated area}_{(\alpha, \beta)}(\mu_A) + \text{reduced area}_{(\alpha, \beta)}(\mu_A) = \text{shadowed area}_{(\alpha, \beta)}(\mu_A) \quad (7)$$

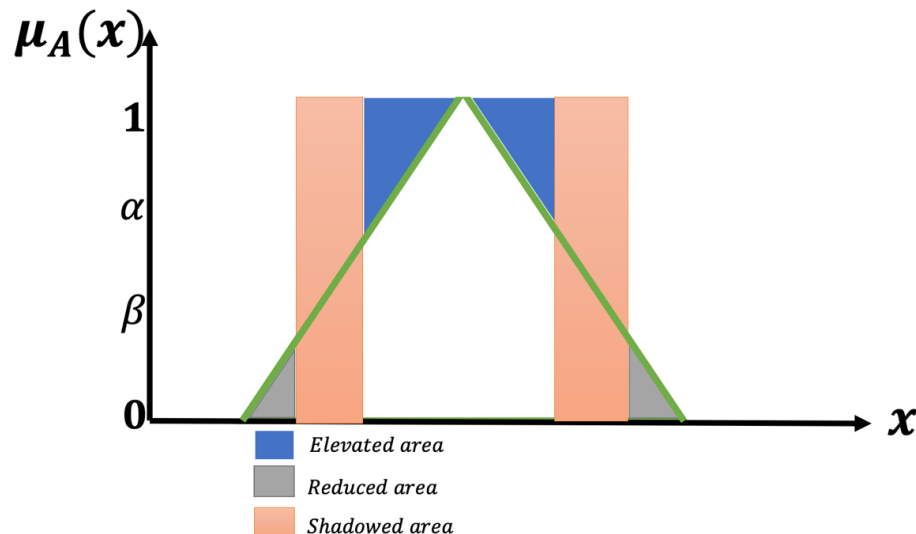


**Figure 3.** Illustration of the shadowed set.

Moreover, the optimal  $\alpha$  and  $\beta$  values are obtained by the optimization of the  $V(\alpha, \beta)$  function described in Equation (8).

$$V(\alpha, \beta) = \left| \int_{x \in A_r} \mu_A(x) dx + \int_{x \in A_e} (1 - \mu_A(x)) dx - \int_{x \in S} dx \right| \quad (8)$$

### 3. Differential Evolution

The differential evolution (DE) algorithm is a population-based stochastic search strategy that was proposed in 1995 by Storn and Price. Its main purpose is to solve optimization problems involving real parameters.

In the literature, several works utilizing DE can be discussed as follows: the differential evolution (DE) algorithm is considered to be a practical and effective method for numerical optimization. It is known for its ease of understanding, simplicity of implementation, reliability, and efficiency. This article attempts to comprehensively describe DE, providing illustrations, valuable insights, and empirical advice. It acknowledges that globally optimal solutions are often challenging to obtain, with many problems being intractable [41].

When dealing with functions that have numerous interacting local optima, the application of fuzzy sets in the job-shop scheduling problem (JSP) with fuzzy processing time and completion time (FJSP) allows for a more comprehensive modeling of scheduling. Fuzzy relative entropy provides a method for evaluating the quality of a feasible solution

by comparing the actual value with the ideal value, which is the due date. Consequently, the multi-objective FJSP can be transformed into a single-objective optimization problem that can be solved using a hybrid adaptive differential evolution (HADE) algorithm. This algorithm considers the maximum completion time, total delay time, and total energy consumption of jobs as optimization criteria. HADE employs a mutation strategy based on DE/current-to-best and makes its parameters (CR and F) adaptive and normally distributed. The selection of new individuals in HADE is based on the fitness value (FRE) obtained from a population consisting of N parents and N children [42]. Maximizing the traffic capacity of an intersection and reducing the delay rate of vehicles have always been challenges in traffic control research. The coordinated control of urban traffic signals is considered a multi-objective optimization problem. In this study, we examine a mathematical model for urban trunk traffic. We establish models for average delay, average queue length, total delay calculation at intersections, and vehicle exhaust emissions to formulate an optimization model for a new coordinated control system for traffic trunks. To address this, a study that combines fuzzy control theory with the adaptive sequencing mutation multi-objective differential evolution algorithm (FASM-MDEA) was offered in [43].

In our proposed model, we utilize two well-known statistical methods, the Pearson correlation coefficient and one-way analysis of variance, to select cost adjustment factors that have a high correlation with the actual effort. Subsequently, we employ the fuzzy C-means clustering algorithm with three cluster heads to group similar projects in the COCOMO-81 dataset. Furthermore, we utilize an improved self-adaptive differential evolution algorithm to optimize the parameters of the constructive cost model [44].

This paper focuses on the use of differential evolution to improve the approximation properties of function approximation models based on fuzzy partitions. Two cases are considered, fuzzy transform and fuzzy projection, and the design of hybrid evolutionary fuzzy systems is studied. Even though function approximation techniques based on fuzzy partitions have been well studied, few papers consider the problem of centroid selection of the basic functions. Thus, in most cases, uniform fuzzy partitions are considered. By using an evolutionary algorithm, a systematic approach on the selection of the partition is provided. The optimization problem involves the determination of the model parameters, which, in our case, are the fuzzy partition's membership functions' locations [45].

Type-3 fuzzy theory is a recent proposal in the literature. In a recent work, a study by varying an important element of interval type-3 fuzzy sets, known as the LowerScale ( $\lambda$ ) parameter, was performed. By manipulating this parameter, different proposed fuzzy systems are utilized to dynamically adjust a parameter of the differential evolution algorithm during its execution, aiming to enhance its convergence [46].

Although DE is considered an algorithm with an exceptionally simple evolutionary strategy, it also proves to be significantly fast and robust. It relies on a small number of parameters, namely:

NP: the number of parent vectors, corresponding to the population size or the number of individuals.

F: the mutation factor or scale factor, typically chosen from the range [0,1].

CR: the recombination factor or crossover rate.

G: the maximum number of generations to be executed.

The performance of the algorithm is highly sensitive to these control values, and each problem may exhibit different responses to different parameter settings.

The mathematical form of DE is expressed by the equations described in the following sections.

### 3.1. Population Size

DE's implementation, known for its versatility, consists of two vector populations. Each population contains  $N_p$  D-dimensional vectors with real-valued parameters. The

current population denoted as  $P_x$  is comprised of vectors  $x_{i,g}$  that have been deemed acceptable either as initial points or through comparison with other vectors.

$$P_{x,g} = (x_{i,g}), i = 0, 1, \dots, Np - 1, g = 0, 1, \dots, g_{max}, \quad (9)$$

$$x_{i,g} = (x_{j,i,g}), j = 0, 1, \dots, D - 1, \quad (10)$$

Indices start with 0 to simplify working with arrays and modular arithmetic. The index,  $g = 0, 1, \dots, g_{max}$ , indicates the generation to which a vector belongs. In addition, each vector is assigned a population index,  $i$ , which runs from 0 to  $Np - 1$ . Parameters within vectors are indexed with  $j$ , which runs from 0 to  $D - 1$ . Once initialized, DE mutates randomly chosen vectors to produce an intermediary population,  $P_{v,g}$ , of  $Np$  mutant vectors,  $v_{i,g}$ :

$$P_{v,g} = (v_{i,g}), i = 0, 1, \dots, Np - 1, g = 0, 1, \dots, g_{max}, \quad (11)$$

$$v_{i,g} = (v_{j,i,g}), j = 0, 1, \dots, D - 1, \quad (12)$$

Each vector in the current population undergoes recombination with a mutant vector, resulting in the creation of a trial population,  $P_u$ , comprising  $Np$  mutant vectors  $u_{i,g}$ .

$$P_{u,g} = (u_{i,g}), i = 0, 1, \dots, Np - 1, g = 0, 1, \dots, g_{max}, \quad (13)$$

$$u_{i,g} = (u_{j,i,g}), j = 0, 1, \dots, D - 1 \quad (14)$$

where:

$P_x$ : current population.

$i$ : index of the population.

$g_{max}$ : maximum number of iterations.

$j$ : parameters within the vector.

During recombination, trial vectors replace the mutant population, allowing a single array to hold both populations.

Initialization of the population requires specifying upper and lower bounds for each parameter. These bounds are collected into two  $D$ -dimensional initialization vectors,  $b_L$  and  $b_U$ , where subscripts L and U indicate the lower and upper bounds, respectively. Using a random number generator, each parameter of every vector is assigned a value within the specified range. For instance, the initial value (at  $g = 0$ ) of the  $j$ th parameter of the  $i$ th vector is determined as:

$$x_{j,i,0} = rand_j(0,1) \cdot (b_{j,U} - b_{j,L}) + b_{j,L} \quad (15)$$

The random number generator,  $rand_j(0,1)$ , returns a uniformly distributed random number from within the range  $(0,1)$ , i.e.,  $0 \leq rand_j(0,1) < 1$ . The subscript,  $j$ , indicates that a new random value is generated for each parameter. Even if a variable is discrete or integral, it should be initialized with a real value since DE internally treats all variables as floating-point values regardless of their type.

### 3.2. Mutation

Specifically, the differential mutation utilizes a random sampling equation to combine three randomly chosen vectors and create a mutant vector.

$$v_{i,g} = x_{r_0,g} + F \cdot (x_{r_1,g} - x_{r_2,g}) \quad (16)$$

The scale factor,  $F \in (0,1)$  is a positive real number that controls the rate at which the population evolves.

### 3.3. Crossover

To complement the differential mutation search strategy, DE also uses uniform crossover. Sometimes this is known as discrete recombination. In particular, DE crosses each vector with a mutant vector as indicated by the following expression:

$$u_{i,g} = u_{j,i,g} \begin{cases} v_{j,i,g} & \text{if } (\text{rand}_j(0,1) \leq Cr \text{ or } j = j_{\text{rand}}) \\ x_{j,i,g} & \text{otherwise} \end{cases} \quad (17)$$

### 3.4. Selection of the Best Individual

If the test vector  $u_{i,g}$  has a value for the objective function equal to or less than its target vector,  $x_{i,g}$ , then it replaces the target vector in the next generation; otherwise, the target retains its place in the population for at least another generation:

$$x_{i,g+1} = \begin{cases} u_{i,g} & \text{if } f(u_{i,g}) \leq f(x_{i,g}) \\ x_{i,g} & \text{otherwise} \end{cases} \quad (18)$$

The process of mutation, recombination and selection are repeated until the optimum is found, or a pre-specified terminating criterion is satisfied.

## 4. Proposed Shadowed Fuzzy using DE Algorithm

The main contribution of this article is the utilization of a novel optimization technique, shadowed type-2 fuzzy systems (ST2-FS), for dynamically adapting the crossover parameter of differential evolution (DE). This adaptation aims to enhance the performance of the DE algorithm when applied to optimize the motor position control problem with interval type-2, specifically by identifying the optimal structure of the membership functions.

Figure 4 displays a flowchart illustrating the procedure employed in this article's general proposal. It demonstrates the utilization of ST2-FS to dynamically adjust the CR parameter, followed by its simulation in the motor controller featuring an IT2-FS.

The equations utilized for constructing the fuzzy parameters of the input and output are presented in Equations (19) and (20), respectively.

$$\text{Generations} = \frac{\text{Current Generation}}{\text{Maximun of generations}} \quad (19)$$

$$\text{CR} = \frac{\sum_{i=1}^{r_{\text{CR}}} \mu_i^{\text{CR}}(\text{CR}_{1i})}{\sum_{i=1}^{r_{\text{CR}}} \mu_i^{\text{CR}}} \quad (20)$$

The number of rules in the fuzzy system for CR is denoted by  $r_{\text{CR}}$ ;  $\text{CR}_{1i}$ , represents the output result for rule  $i$  of CR, while  $\mu_i^{\text{CR}}$ , represents the membership function (MF) of rule  $i$  of CR.

The fuzzy system structure integrated into the DE algorithm consists of the following characteristics. We refer to the combination of ST2-FS with the DE algorithm as DE-ST2-FS. The system comprises an input representing the generations used in the DE algorithm, and the output is the CR parameter that represents the crossover. In the original algorithm, this parameter is defined within the range of [0,1]. Both the input and output are divided into three membership functions (MFs), as depicted in Figure 5.

The rules that form the fuzzy system are presented below. These rules were developed based on experimentation, which demonstrated that decreasing the CR parameter during the algorithm's execution yields favorable results.

1. If generation is low, then CR is low.
2. If generation is medium, then CR is medium.
3. If generation is high, then CR is high.

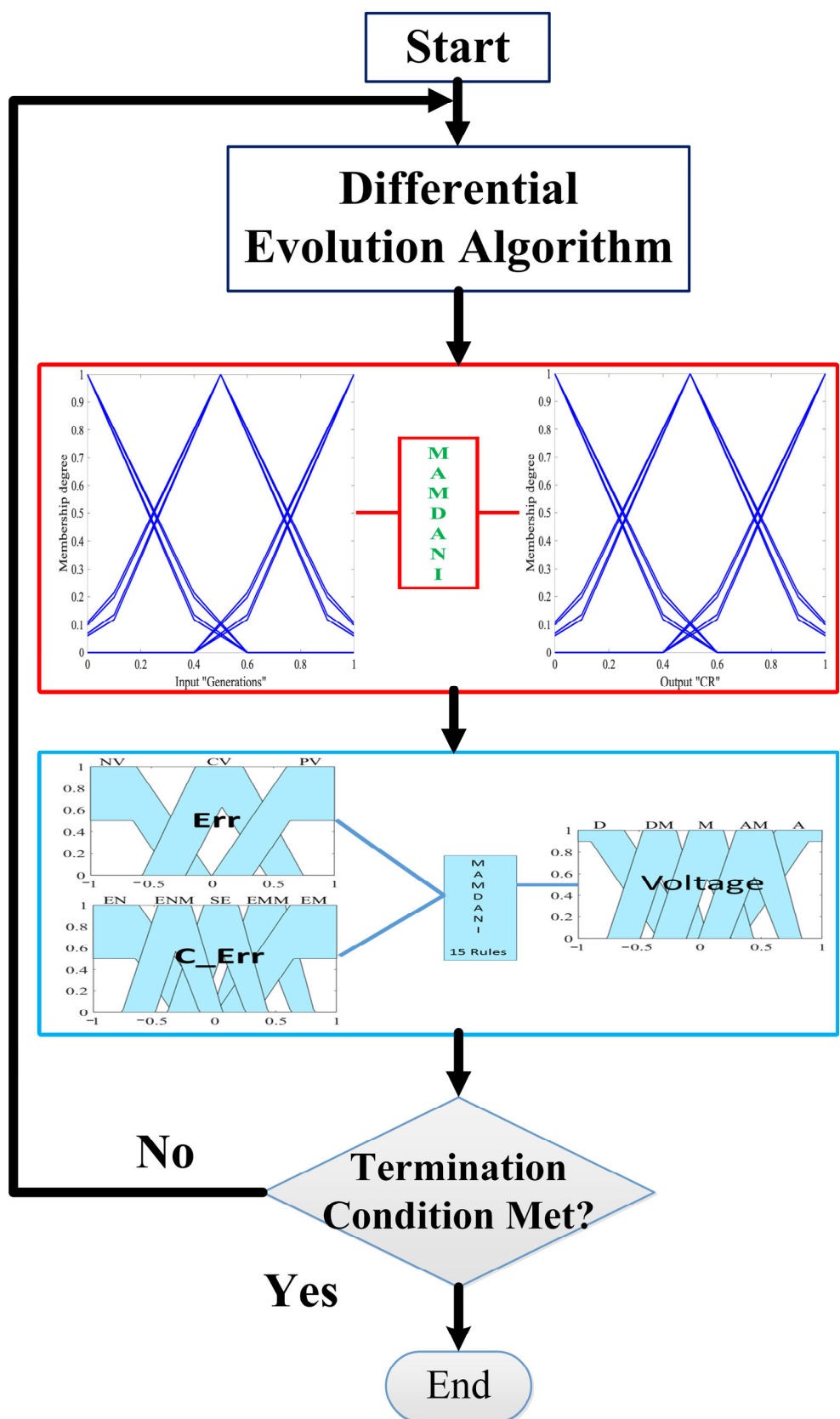


**Figure 4.** Proposal flowchart.

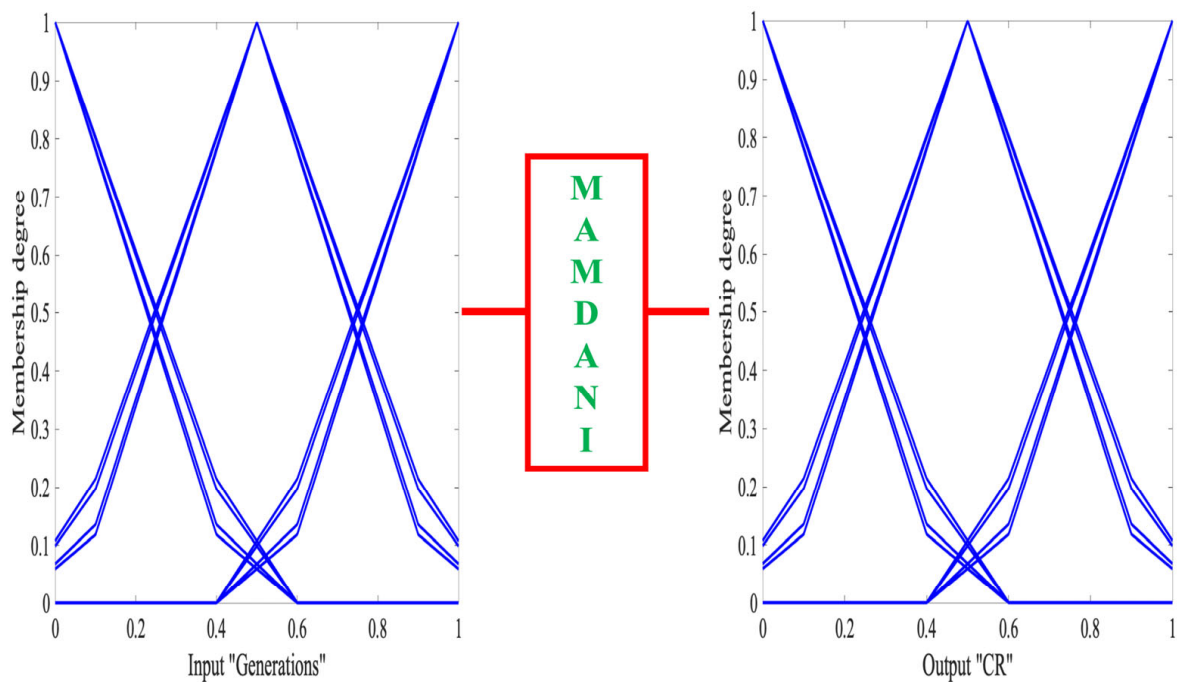


**Figure 5.** Shadowed fuzzy system integrated with the DE algorithm (DE-ST2-FS).

##### 5. Interval Type-2 Fuzzy Systems Controller

Position control of a direct current (DC) motor is a circuit capable of controlling the position of any DC motor with the simple movement of a potentiometer that acts as a positioner, and it does so through proportional control [47–50]. One of the purposes of this work is the optimization of the interval type-2 fuzzy controller, which we will call (IT2-FLC), which is structured as illustrated in Figure 6.

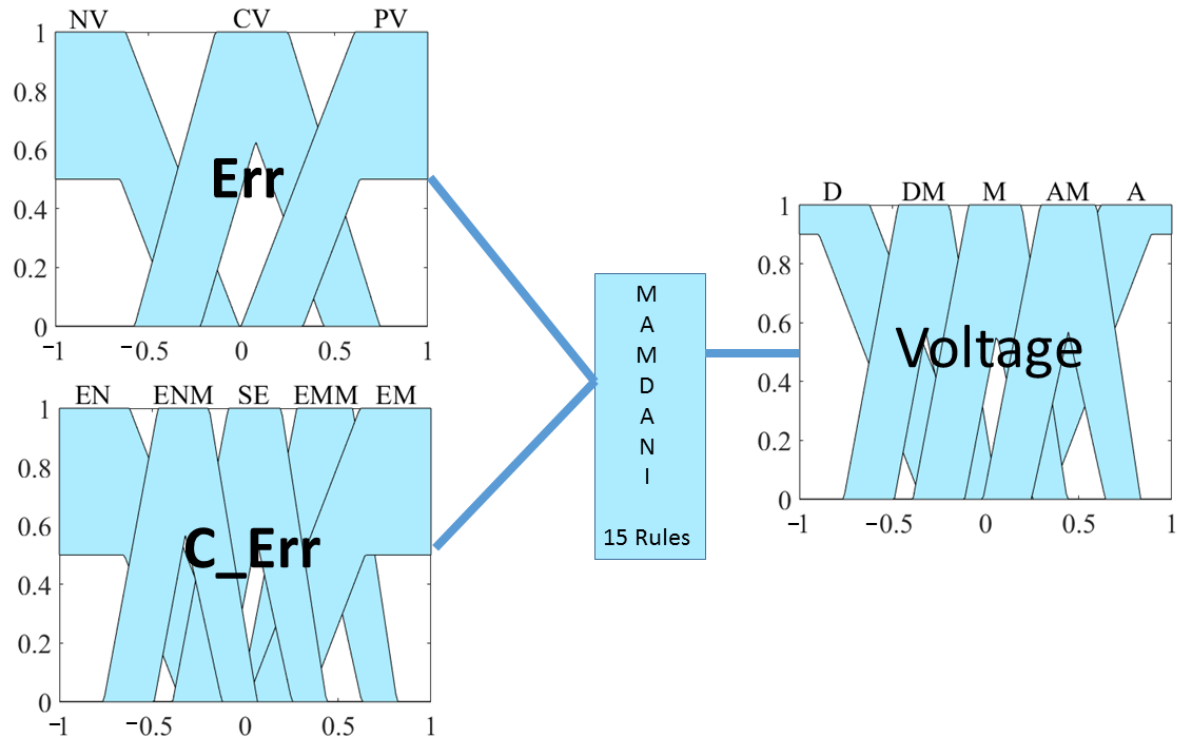


**Figure 6.** IT2-FLC controller.

The fuzzy system is defined as: the inputs are the error “Err” and the error change “C\_Err”, the output corresponds to the voltage “Voltage”, the “Err” input contains three MFs, the ends are of type “trapIT2mf”, and the center is “triIT2mf”. The equations that describe the knowledge of each function are shown in Equations (21) and (22).

The second input “C\_Err” contains five membership functions, the ends are of type “trapIT2mf”, and the three central functions are of type “triIT2mf”.

Finally, the output “Voltage” consists of five membership functions, the ends are of type “trapIT2mf”, and the three central functions are of type “triIT2mf”.

$$\begin{aligned} trapIT2mf(x, [a_1, b_1, c_1, d_1, a_2, b_2, c_2, d_2, \alpha]) \\ = \begin{cases} a_1 < a_2, b_1 < b_2, c_1 < c_2, d_1 < d_2 \\ \mu_1(x) = \max\left(\min\left(\frac{x-a_1}{b_1-a_1}, 1, \frac{d_1-x}{d_1-c_1}\right), 0\right) \\ \mu_2(x) = \max\left(\min\left(\frac{x-a_2}{b_2-a_2}, 1, \frac{d_2-x}{d_2-c_2}\right), 0\right) \\ \mu(x) = \begin{cases} \max(\mu_1(x), \mu_2(x)) & \forall x \notin (b_1, c_2) \\ 1 & \forall x \in (b_1, c_2) \end{cases} \\ \underline{\mu}(x) = \min(\alpha, \min(\mu_1(x), \mu_2(x))) \end{cases} \quad (21) \end{aligned}$$

$$\begin{aligned} triIT2mf(x, [a_1, b_1, c_1, a_2, b_2, c_2]) \\ = \begin{cases} a_1 < a_2, b_1 < b_2, c_1 < c_2 \\ \mu_1(x) = \max\left(\min\left(\frac{x-a_1}{b_1-a_1}, \frac{c_1-x}{c_1-b_1}\right), 0\right) \\ \mu_2(x) = \max\left(\min\left(\frac{x-a_2}{b_2-a_2}, \frac{c_2-x}{c_2-b_2}\right), 0\right) \\ \mu(x) = \begin{cases} \max(\mu_1(x), \mu_2(x)) & \forall x \notin (b_1, b_2) \\ 1 & \forall x \in (b_1, b_2) \end{cases} \\ \underline{\mu}(x) = \min(\mu_1(x), \mu_2(x)) \end{cases} \quad (22) \end{aligned}$$

IT2-FLC rules are outlined in Table 1.

**Table 1.** IT2-FLC rules.

		C_Err				
		EN	ENM	SE	EMM	EM
Err	NV	D	D	D	D	DM
	CV	AM	AM	M	DM	DM
	PV	AM	A	A	A	A

## 6. Results and Statistical Comparison

In this section, we are presenting the experimentation that were performed, the parameters used, and the objective function used for the experimentation.

The root means square error (RMSE) represents the objective function for our experimentation, where we seek to measure the difference between the desired and the obtained in the controller. The formula that represents the RMSE is described in Equation (23), where  $x_t$  is the estimated value of the reference control signal,  $\hat{x}_t$  is the observed value control-signal, and  $N$  represents the total number of observed samples.

$$RMSE = \sqrt{\frac{1}{N} \sum_{t=1}^N (x_t - \hat{x}_t)^2} \quad (23)$$

The parameters that involve the experimentation of the DE-ST2-FS algorithm are described in Table 2, where we can importantly rescue the parameter CR that is dynamic due to the ST2-FS.

**Table 2.** Parameter configuration of the DE-ST2-FS.

Parameter Configuration	
NP	20
D	25
GEN	20
F	0.5
CR	Dynamic
Number of experiments	30

The conducted experimentation is summarized in Table 3, which demonstrates the usage of the DE-ST2-FS proposal without applying noise to the controller. Subsequently, the performance of a type-2 controller in handling intervals was evaluated by introducing Gaussian random noise at three different levels: 0.3, 0.5, and 0.9.

**Table 3.** DE-ST2-FS fuzzy system.

	DE-ST2-FS without Noise	DE-ST2-FS with Noise 0.5	DE-ST2-FS with Noise 0.7	DE-ST2-FS with Noise 0.9
Min.	$5.48 \times 10^{-1}$	$5.28 \times 10^{-1}$	$9.38 \times 10^{-2}$	$1.31 \times 10^{-2}$
Max.	$6.08 \times 10^{-1}$	$6.01 \times 10^{-1}$	$9.78 \times 10^{-2}$	$7.63 \times 10^{-2}$
Average	$5.99 \times 10^{-1}$	$5.63 \times 10^{-1}$	$9.58 \times 10^{-2}$	$5.92 \times 10^{-2}$
Standard D.	$1.23 \times 10^{-2}$	$1.55 \times 10^{-2}$	$6.22 \times 10^{-4}$	$2.15 \times 10^{-2}$

An analysis of Table 4 shows that the utilization of the controller with a noise level of 0.5 is better in terms of minimum error compared to the proposal without applying noise to the controller.

**Table 4.** Z-test parameters.

Parameter	Value
Level of Confidence	95%
Alpha $\alpha$	5%
$H_a$	$\mu_1 < \mu_2$
$H_o$	$\mu_1 \geq \mu_2$
Critical Value	-1.645

On the other hand, it is also observed that, in comparison to the minimum error, a better result is obtained when a noise level of 0.9 is applied compared to a noise level of 0.7.

Regarding the averages of the experimentation, they all have the same order, but it can be observed how the average decreases when the noise level increases.

Figure 7 shows a comparison of the experimentation with the different noise levels.

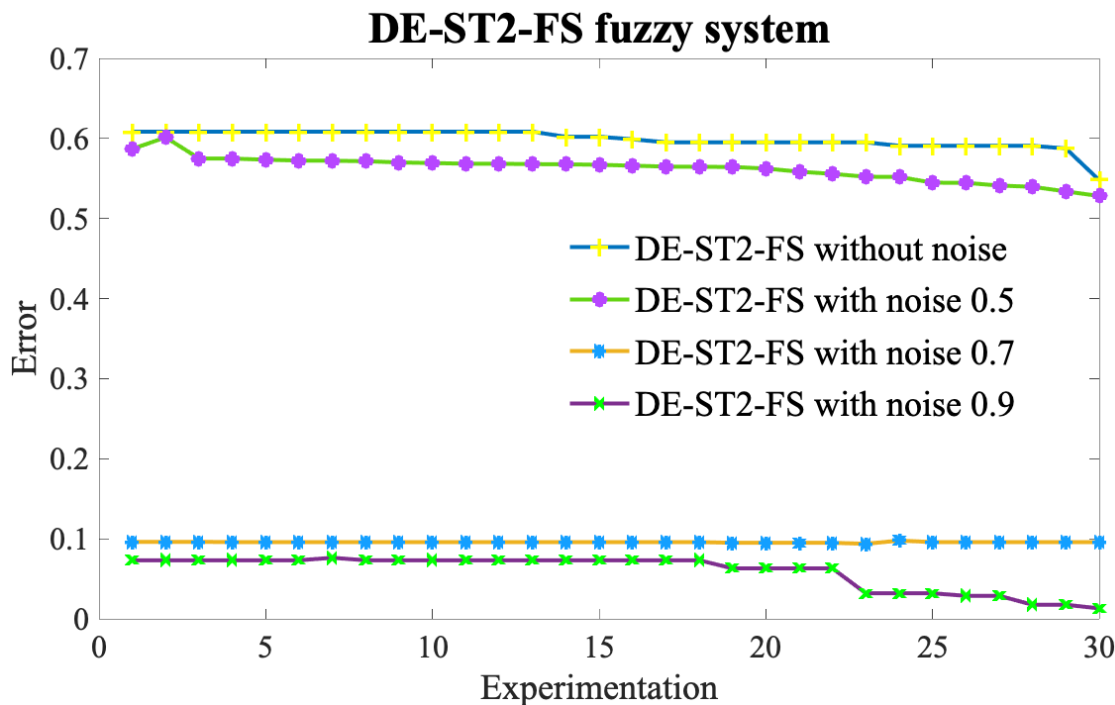
The analysis of Figure 7 shows us that with a higher noise level, the DE-ST2-FS proposal shown in this work obtains better results; however, not applying noise to the DE-ST2-FS controller has a similar behavior to DE-ST2-FS with noise 0.5, while DE-ST2-FS with noise 0.7 and DE-ST2-FS with noise 0.9 have very similar behaviors. Overall, a better result is observed with DE-ST2-FS with noise 0.9.

The results of the minimum values obtained in Table 4 are represented in Figures 8–11, showcasing the four different experimental scenarios: DE-ST2-FS without noise, DE-ST2-FS with noise 0.5, DE-ST2-FS with noise 0.7, and DE-ST2-FS with noise 0.9.

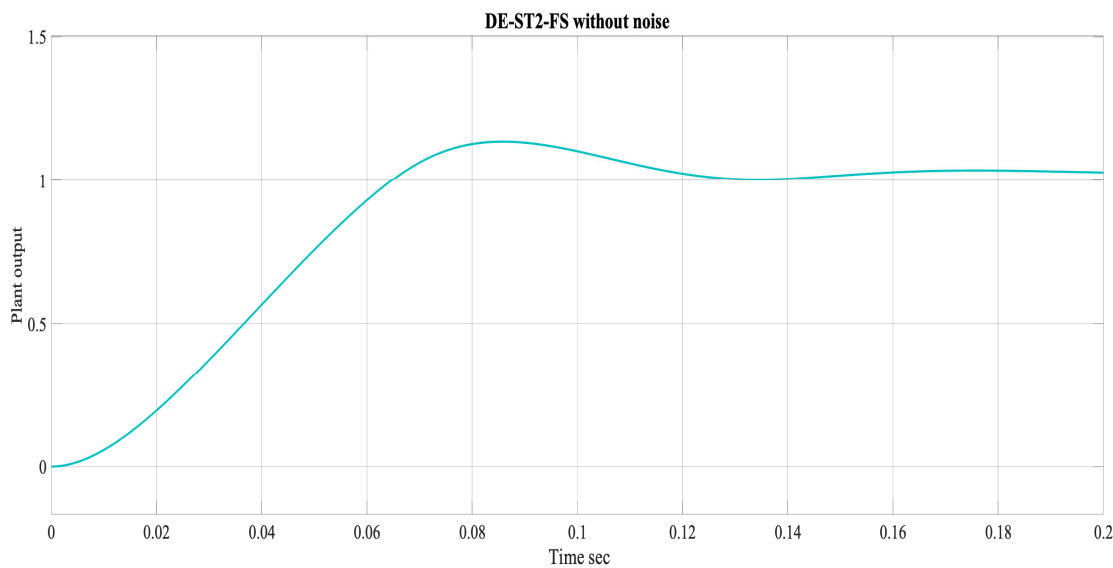
Figure 8 shows the minimum RMSE of the simulation of the 30 experiments performed with DEST2-FS without noise, where the value obtained was  $5.48 \times 10^{-1}$ . In Figure 6, when starting the simulation, it exceeds what is desired, but later it stabilizes in the second 0.12 to 0.14 and later it exceeds again from the second 0.14 to 0.2.

Figure 9 illustrates the minimum RMSE of the simulation of the 30 experiments carried out with DE-ST2-FS with noise 0.5, where the value obtained was  $5.28 \times 10^{-1}$ . In the figure, when starting the simulation, it exceeds between seconds 0.06 and 0.1, later a stabilization is observed from second 0.16 to 0.2.

Figure 10 shows the minimum RMSE of the simulation of the 30 experiments carried out with DE-ST2-FS with noise 0.7, where the value obtained was  $9.38 \times 10^{-2}$ . In the figure, the controller has stability from 0.1 s to 0.16 s, while between 0.16 s and 0.2 s the controller output drifts slightly from the desired reference.



**Figure 7.** Graphical comparison of experimentation.



**Figure 8.** Best result DE-ST2-FS without noise.

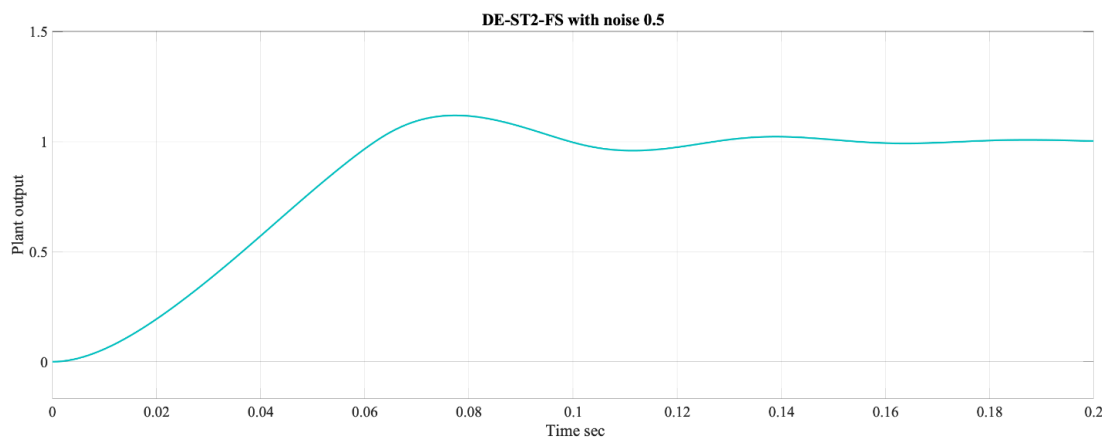


**Figure 9.** Best result DE-ST2-FS with noise 0.5.

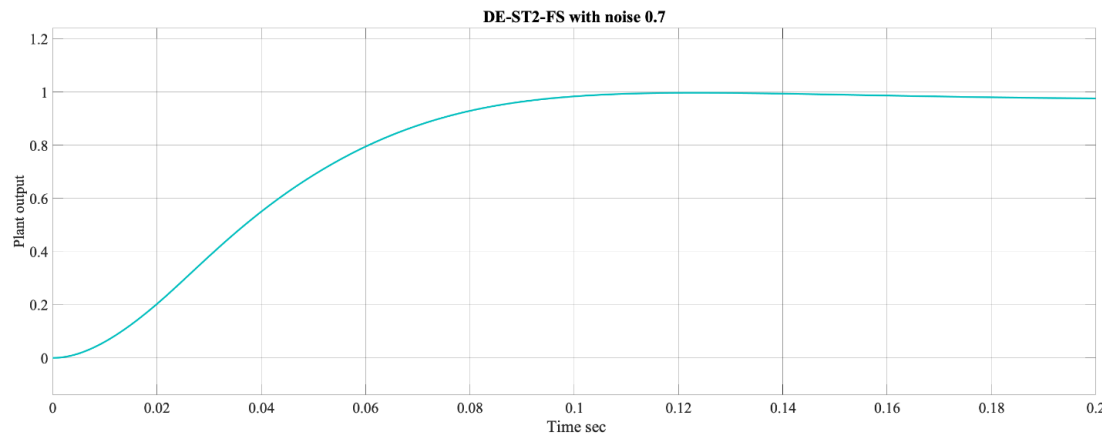


**Figure 10.** Best result DE-ST2-FS with noise 0.7.

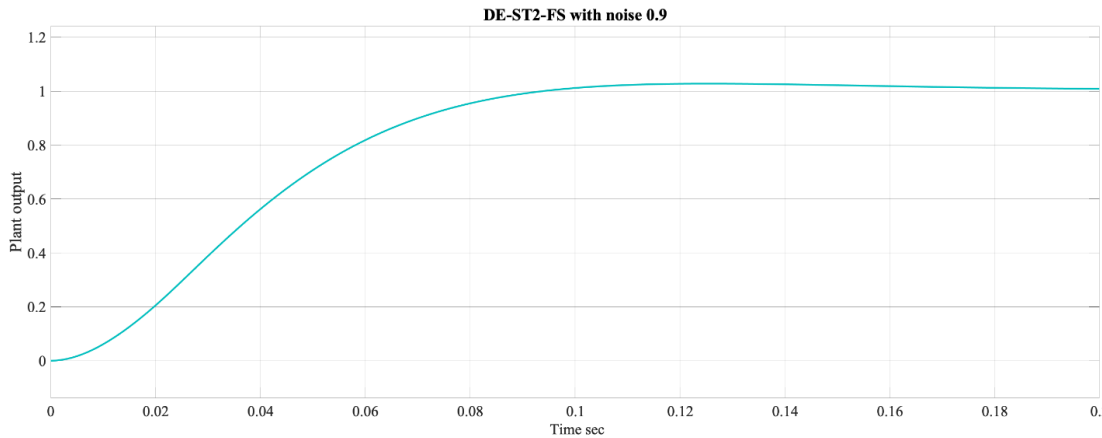


**Figure 11.** Best result DE-ST2-FS with noise 0.9.

Finally, Figure 11 shows the RMSE of the simulation of the 30 experiments carried out with DE-ST2-FS with noise 0.9, where the value obtained was  $1.31 \times 10^{-2}$ . In the simulation obtained, it is observed that from second 0.1 the output of the plant has stability, but in between seconds 0.16 and 0.2 it is possible to stabilize.

In order to demonstrate that better results are obtained when using DE-ST2-FS with a high noise level, a statistical test was performed. The statistic used in this work is the

Z-test, the parameters used are shown in Table 4, and Equation (24) was used to calculate the Z value.

$$Z = \frac{(\bar{X}_1 - \bar{X}_2) - (\mu_1 - \mu_2)}{\sigma_{\bar{X}_1 - \bar{X}_2}} \quad (24)$$

The objective of the statistical test is to show that DE-ST2-FS with noise 0.9 has a lower average than the other three variants of experimentation carried out: DE-ST2-FS without noise, DE-ST2-FS with noise 0.5, and DE-ST2-FS with noise 0.7.

Three statistical tests were performed, where  $\mu_1$  is equal to DE-ST2-FS with noise 0.9 and  $\mu_2$  represents each of the statistical tests carried out. The results of the tests are outlined in Table 5.

**Table 5.** Z-test results.

Case Study	$\mu_1$	$\mu_2$	Z Value	Evidence
Controller	DE-ST2-FS with noise 0.9	DE-ST2-FS without noise	-119.3636	Significant
	DE-ST2-FS with noise 0.9	DE-ST2-FS with noise 0.5	-104.1108	Significant
	DE-ST2-FS with noise 0.9	DE-ST2-FS with noise 0.7	-9.3201	Significant

The results of the tests show that the greater the uncertainty, the better results are obtained. The three statistical tests carried out show that DE-ST2-FS with noise 0.9 has a lower average than the other three proposals carried out.

Next, a comparison was made with other works found in the literature, in order to be able to validate the proposal to make CR dynamic in the DE and having an interval type-2 controller.

We use as reference “Shadowed Type-2 Fuzzy Systems for Dynamic Parameter Adaptation in Harmony Search and Differential Evolution” [51]. In this previous work, two metaheuristics are used, where one of the parameters is dynamically adapted with a ST2-FS, and the difference with the reference is that the controller used is a T1-FS compared to ours, which is an IT2-FS.

Table 6 exhibits the results from the literature and the results of the best experiments carried out in our work with ST2-FS with noise 0.9, reporting the averages and standard deviations.

**Table 6.** DE-ST2FS with noise 0.9 comparison.

	ST2FHS-FLC FLC with Noise [51]	ST2FDE-FLC with Noise [51]	DE-ST2-FS with Noise 0.9
Average	$4.62 \times 10^{-1}$	$2.1 \times 10^{-2}$	$5.92 \times 10^{-2}$
Standard D.	$2.83 \times 10^{-2}$	$1.90 \times 10^{-2}$	$2.15 \times 10^{-2}$

Using the data from Table 6, two statistical tests were performed to check if our proposal has a lower average than other methods in the literature. The previously shown Z-test was used, according to Equation (23), and the same parameters used in Table 4 were employed.

For the statistical test,  $\mu_1$  is equal to DEST2-FS with noise 0.9 and  $\mu_2$  is equal to the two different methods ST2FHS-FLC with Noise and ST2FDE-FLC with Noise [51]. Table 7 reports the Z-test results for the two tests.

The test results indicate that we have sufficient significant evidence to conclude that DE-ST2-FS with noise 0.9 has a lower average than ST2FHS-FLC with Noise. However, for the second statistical test, we do not have enough significant evidence to claim that DE-ST2-FS with noise 0.9 has a lower average than ST2FDE-FLC with Noise.

**Table 7.** Statistical Z-test results.

Case Study	$\mu_1$	$\mu_2$	Z Value	Evidence
Controller	DE-ST2-FS with noise 0.9	ST2FHS-FLC FLC with Noise [51]	−62.0761	Significant
	DE-ST2-FS with noise 0.9	ST2FDE-FLC with Noise [51]	7.1395	Not Significant

## 7. Conclusions

For our conclusions, the main contribution is the use of the dynamic CR parameter in differential evolution, as well as the ST2-FS, as this combination is new and there are no current works that utilize our DE-ST2-FS proposal.

This work demonstrates that the use of uncertainty improves the obtained results. In the DE-ST2-FS proposal we used the ST2-FS controller without applying noise and later the noise level was increased in order to demonstrate that at higher noise levels, the IT2-FLC has better stability. The statistical test supports that DE-ST2-FS with noise 0.9 has a lower average than DE-ST2-FS without noise, DE-ST2-FS with noise 0.5, and DE-ST2-FS with noise 0.7.

Figures 8–11 illustrate the improvement achieved by increasing the noise level, as they display the minimum RMSE obtained from each of the different experiments. The comparison with the two methods, namely ST2FHS-FLC with Noise and ST2FDE-FLC with Noise, reveals that our proposal exhibits a lower average than ST2FHS-FLC with Noise. However, we did not obtain significant evidence in favor of our proposal compared to ST2FDE-FLC with Noise. In the latter case, the reference method utilizes a ST2-FS, which makes the F (mutation) parameter of the differential evolution algorithm dynamic. We believe that this is the reason why we lack significant evidence in our proposal. Previous works have statistically confirmed that making the F parameter dynamic yields better results than making the CR parameter dynamic.

**Author Contributions:** C.P., P.O. and O.C. conducted the state-of-the-art review, literature review, and developed the main idea. O.C. and Z.W.G. provided supervision. All authors have read and agreed to the published version of the manuscript.

**Funding:** This research received no external funding.

**Data Availability Statement:** Not applicable.

**Acknowledgments:** We would like to thank the Tijuana Institute of Technology and TecNM for their support.

**Conflicts of Interest:** The authors declare no conflict of interest.

## References

- Rossi, F.; Sembiring, J.P.; Jayadi, A.; Putri, N.U.; Nugroho, P. Implementation of Fuzzy Logic in PLC for Three-Story Elevator Control System. In Proceedings of the 2021 International Conference on Computer Science, Information Technology, and Electrical Engineering (ICOMITEE), Banyuwangi, Indonesia, 27–28 October 2021; pp. 179–185. [[CrossRef](#)]
- Krishnan, R.S.; Julie, E.G.; Robinson, Y.H.; Raja, S.; Kumar, R.; Thong, P.H.; Son, L.H. Fuzzy Logic based Smart Irrigation System using Internet of Things. *J. Clean. Prod.* **2019**, *252*, 119902. [[CrossRef](#)]
- Belman-Flores, J.M.; Rodríguez-Valderrama, D.A.; Ledesma, S.; García-Pabón, J.J.; Hernández, D.; Pardo-Cely, D.M. A Review on Applications of Fuzzy Logic Control for Refrigeration Systems. *Appl. Sci.* **2022**, *12*, 1302. [[CrossRef](#)]
- Chen, X.; Hu, Z.; Sun, Y. Fuzzy Logic Based Logical Query Answering on Knowledge Graphs. *Proc. Conf. AAAI Artif. Intell.* **2022**, *36*, 3939–3948. [[CrossRef](#)]
- Almadi, A.I.M.; Al Mamlook, R.E.; Almarhabi, Y.; Ullah, I.; Jamal, A.; Bandara, N. A Fuzzy-Logic Approach Based on Driver Decision-Making Behavior Modeling and Simulation. *Sustainability* **2022**, *14*, 8874. [[CrossRef](#)]
- Zhao, Z.-H. Improved fuzzy logic control-based energy management strategy for hybrid power system of FC/PV/battery/SC on tourist ship. *Int. J. Hydrogen Energy* **2022**, *47*, 9719–9734. [[CrossRef](#)]
- Kenjrawy, H.; Makdisie, C.; Houssamo, I.; Mohammed, N. New Modulation Technique in Smart Grid Interfaced Multilevel UPQC-PV Controlled via Fuzzy Logic Controller. *Electronics* **2022**, *11*, 919. [[CrossRef](#)]

8. Atoui, A.; Boucherit, M.S.; Benmansour, K.; Barkat, S.; Djeriou, A.; Houari, A. Unified fuzzy logic controller and power management for an isolated residential hybrid PV/diesel/battery energy system. *Clean Energy* **2022**, *6*, 671–681. [[CrossRef](#)]
9. Zhu, Y.; Wang, Z.; Guo, X.; Wei, Z. An improved kinetic energy control strategy for power smoothing of PMSG-WECS based on low pass filter and fuzzy logic controller. *Electr. Power Syst. Res.* **2023**, *214*, 108816. [[CrossRef](#)]
10. Afaq, M.; Jebelli, A.; Ahmad, R. An Intelligent Thermal Management Fuzzy Logic Control System Design and Analysis Using ANSYS Fluent for a Mobile Robotic Platform in Extreme Weather Applications. *J. Intell. Robot. Syst.* **2023**, *107*, 11. [[CrossRef](#)]
11. Ahmad, I.; M’Zoughi, F.; Aboutalebi, P.; Garrido, I.; Garrido, A.J. Fuzzy logic control of an artificial neural network-based floating offshore wind turbine model integrated with four oscillating water columns. *Ocean Eng.* **2023**, *269*, 113578. [[CrossRef](#)]
12. Moutchou, R.; Abbou, A.; Jabri, B.; Rhaili, S.E.; Chigane, K. Adaptive Fuzzy Logic Controller for MPPT Control in PMSG Wind Turbine Generator. In *Artificial Intelligence-Based Smart Power Systems*; IEEE Press: Piscataway, NJ, USA, 2022; pp. 129–140. [[CrossRef](#)]
13. Wang, X.; Xu, B.; Guo, Y. Fuzzy Logic System-Based Robust Adaptive Control of AUV with Target Tracking. *Int. J. Fuzzy Syst.* **2022**, *25*, 338–346. [[CrossRef](#)]
14. Liu, J.; Wei, T.; Chen, N.; Wu, J.; Xiao, P. Fuzzy Logic PID Controller with Both Coefficient and Error Modifications for Digitally-Controlled DC–DC Switching Converters. *J. Electr. Eng. Technol.* **2023**, *1*–12. [[CrossRef](#)]
15. Vijayalakshmi, K.; Kn, S. Intelligent Control of Switched Reluctance Motor Using Fuzzy Logic and SMC Controller for EV Applications. *Int. J. Eng. Educ.* **2023**, *4*, 42–57. [[CrossRef](#)]
16. Tan, D.W.W.W. A simplified type-2 fuzzy logic controller for real-time control. *ISA Trans.* **2006**, *45*, 503–516. [[CrossRef](#)]
17. Castillo, O.; Aguilar, L.; Cázares, N.; Cárdenas, S. Systematic design of a stable type-2 fuzzy logic controller. *Appl. Soft Comput.* **2008**, *8*, 1274–1279. [[CrossRef](#)]
18. Wu, D.; Tan, W. A type-2 fuzzy logic controller for the liquid-level process. In Proceedings of the 2004 IEEE International Conference on Fuzzy Systems (IEEE Cat. No. 04CH37542), Budapest, Hungary, 25–29 July 2005; IEEE Press: Piscataway, NJ, USA, 2005. [[CrossRef](#)]
19. Zhang, Q.; Wang, Y.; Cheng, J.; Yan, H.; Shi, K. Improved filtering of interval type-2 fuzzy systems over Gilbert-Elliott channels. *Inf. Sci.* **2023**, *627*, 132–146. [[CrossRef](#)]
20. Bernal, E.; Lagunes, M.L.; Castillo, O.; Soria, J.; Valdez, F. Optimization of Type-2 Fuzzy Logic Controller Design Using the GSO and FA Algorithms. *Int. J. Fuzzy Syst.* **2020**, *23*, 42–57. [[CrossRef](#)]
21. Sain, D.; Praharaj, M.; Bosukonda, M.M. A simple modelling strategy for integer order and fractional order interval type-2 fuzzy PID controllers with their simulation and real-time implementation. *Expert Syst. Appl.* **2022**, *202*, 117196. [[CrossRef](#)]
22. Laib, A.; Talbi, B.; Krama, A.; Gharib, M. Hybrid Interval Type-2 Fuzzy PID+I Controller for a Multi-DOF Oilwell Drill-String System. *IEEE Access* **2022**, *10*, 67262–67275. [[CrossRef](#)]
23. Saraswat, R.; Suhag, S. Type-2 fuzzy logic PID control for efficient power balance in an AC microgrid. *Sustain. Energy Technol. Assess.* **2023**, *56*, 103048. [[CrossRef](#)]
24. Liu, X.; Zhao, T.; Cao, J.; Li, P. Design of an interval type-2 fuzzy neural network sliding mode robust controller for higher stability of magnetic spacecraft attitude control. *ISA Trans.* **2023**; *in press*. [[CrossRef](#)]
25. Jovanović, A.; Kukić, K.; Stevanović, A.; Teodorović, D. Restricted crossing U-turn traffic control by interval Type-2 fuzzy logic. *Expert Syst. Appl.* **2023**, *211*, 118613. [[CrossRef](#)]
26. Wijayasekara, D.; Linda, O.; Manic, M. Shadowed Type-2 Fuzzy Logic Systems. In Proceedings of the 2013 IEEE Symposium on Advances in Type-2 Fuzzy Logic Systems (T2FUZZ), Singapore, 16–19 April 2013; pp. 15–22. [[CrossRef](#)]
27. Castillo, O.; Peraza, C.; Ochoa, P.; Amador-Angulo, L.; Melin, P.; Park, Y.; Geem, Z.W. Shadowed Type-2 Fuzzy Systems for Dynamic Parameter Adaptation in Harmony Search and Differential Evolution for Optimal Design of Fuzzy Controllers. *Mathematics* **2021**, *9*, 2439. [[CrossRef](#)]
28. Tahayori, H.; Sadeghian, A. Shadowed fuzzy sets: A framework with more freedom degrees for handling uncertainties than interval type-2 fuzzy sets and lower computational complexity than general type-2 fuzzy sets. In *New Concepts and Applications in Soft Computing*; Springer: Berlin/Heidelberg, Germany, 2013; pp. 97–117. [[CrossRef](#)]
29. Zhou, J.; Lai, Z.; Miao, D.; Gao, C.; Yue, X. Multigranulation rough-fuzzy clustering based on shadowed sets. *Inf. Sci.* **2018**, *507*, 553–573. [[CrossRef](#)]
30. El-Hawy, M.A.; Wassif, K.T.; Hefny, H.; Hassan, H.A. A proposed shadowed intuitionistic fuzzy numbers. In Proceedings of the 2015 Tenth International Conference on Computer Engineering & Systems (ICCES), Cairo, Egypt, 23–24 December 2015; pp. 153–160. [[CrossRef](#)]
31. Zadeh, L.A. Fuzzy sets. *Inf. Control* **1965**, *8*, 338–353. [[CrossRef](#)]
32. Wagner, C.; Hagras, H. Toward General Type-2 Fuzzy Logic Systems Based on zSlices. *IEEE Trans. Fuzzy Syst.* **2010**, *18*, 637–660. [[CrossRef](#)]
33. Coupland, S.; John, R. Geometric Type-1 and Type-2 Fuzzy Logic Systems. *IEEE Trans. Fuzzy Syst.* **2007**, *15*, 3–15. [[CrossRef](#)]
34. Mendel, J.M.; Liu, F.; Zhai, D.  $\alpha$ -Plane Representation for Type-2 Fuzzy Sets: Theory and Applications. *IEEE Trans. Fuzzy Syst.* **2009**, *17*, 1189–1207. [[CrossRef](#)]
35. Mendel, J.M.; John, R.I.; Liu, F. Interval Type-2 Fuzzy Logic Systems Made Simple. *IEEE Trans. Fuzzy Syst.* **2006**, *14*, 808–821. [[CrossRef](#)]

36. Ontiveros, E.; Melin, P.; Castillo, O. High order  $\alpha$ -planes integration: A new approach to computational cost reduction of General Type-2 Fuzzy Systems. *Eng. Appl. Artif. Intell.* **2018**, *74*, 186–197. [[CrossRef](#)]
37. Dorantes, P.N.M.; Mendez, G.M. Non-iterative Wagner-Hagras General Type-2 Mamdani Singleton Fuzzy Logic System Optimized by Central Composite Design in Quality Assurance by Image Processing. In *Recent Trends on Type-2 Fuzzy Logic Systems: Theory, Methodology and Applications*; Springer International Publishing: Cham, Switzerland, 2023; pp. 201–216. [[CrossRef](#)]
38. Pedrycz, W. From fuzzy sets to shadowed sets: Interpretation and computing. *Int. J. Intell. Syst.* **2008**, *24*, 48–61. [[CrossRef](#)]
39. Pedrycz, W.; Song, M. Granular fuzzy models: A study in knowledge management in fuzzy modeling. *Int. J. Approx. Reason.* **2012**, *53*, 1061–1079. [[CrossRef](#)]
40. Pedrycz, W.; Vukovich, G. Granular computing in the development of fuzzy controllers. *Int. J. Intell. Syst.* **1999**, *14*, 419–447. [[CrossRef](#)]
41. Price, K.V.; Storn, R.M.; Lampinen, J.A. The differential evolution algorithm. In *Differential Evolution: A Practical Approach to Global Optimization*; Springer: Berlin/Heidelberg, Germany, 2006; pp. 37–134. [[CrossRef](#)]
42. Wang, G.-G.; Gao, D.; Pedrycz, W. Solving Multiobjective Fuzzy Job-Shop Scheduling Problem by a Hybrid Adaptive Differential Evolution Algorithm. *IEEE Trans. Ind. Inform.* **2022**, *18*, 8519–8528. [[CrossRef](#)]
43. Lin, H.; Han, Y.; Cai, W.; Jin, B. Traffic Signal Optimization Based on Fuzzy Control and Differential Evolution Algorithm. *IEEE Trans. Intell. Transp. Syst.* **2022**, *1–12*, accepted. [[CrossRef](#)]
44. Gouda, S.K.; Mehta, A.K. Software cost estimation model based on fuzzy C-means and improved self adaptive differential evolution algorithm. *Int. J. Inf. Technol.* **2022**, *14*, 2171–2182. [[CrossRef](#)]
45. Korkidis, P.; Dounis, A. On training non-uniform fuzzy partitions for function approximation using differential evolution: A study on fuzzy transform and fuzzy projection. *Inf. Sci.* **2023**, *619*, 867–888. [[CrossRef](#)]
46. Ochoa, P.; Castillo, O.; Melin, P.; Castro, J.R. Interval Type-3 Fuzzy Differential Evolution for Parameterization of Fuzzy Controllers. *Int. J. Fuzzy Syst.* **2023**, *25*, 1360–1376. [[CrossRef](#)]
47. Chairez, I.; Utkin, V. Direct Current Motor Position Control by a Sliding Mode Controlled Dual Three-Phase AC-DC Power Converter. *IFAC-PapersOnLine* **2022**, *55*, 333–338. [[CrossRef](#)]
48. Top, A.; Gökbüyük, M. A novel period-based method for the measurement direct current motor velocity using low-resolver encoder. *Trans. Inst. Meas. Control* **2022**, *45*, 711–722. [[CrossRef](#)]
49. Runjing, Z.; Yu, D.; Weiting, Y. Application of Fuzzy-PI Controller with Feedforward Control in Direct Current Motor Servo System. In Proceedings of the 2005 International Conference on Neural Networks and Brain, Beijing, China, 13–15 October 2005; Volume 2, pp. 1262–1267. [[CrossRef](#)]
50. Karabacak, Y.; Uysal, A. Fuzzy logic controlled brushless direct current motor drive design and application for regenerative braking. In Proceedings of the 2017 International Artificial Intelligence and Data Processing Symposium (IDAP), Malatya, Turkey, 16–17 September 2017; pp. 1–7. [[CrossRef](#)]
51. Castillo, O.; Melin, P.; Valdez, F.; Soria, J.; Ontiveros-Robles, E.; Peraza, C.; Ochoa, P. Shadowed Type-2 Fuzzy Systems for Dynamic Parameter Adaptation in Harmony Search and Differential Evolution Algorithms. *Algorithms* **2019**, *12*, 17. [[CrossRef](#)]

**Disclaimer/Publisher’s Note:** The statements, opinions and data contained in all publications are solely those of the individual author(s) and contributor(s) and not of MDPI and/or the editor(s). MDPI and/or the editor(s) disclaim responsibility for any injury to people or property resulting from any ideas, methods, instructions or products referred to in the content.